J Biomol NMR (2016) 65:59–64
DOI 10.1007/s10858-016-0038-9

COMMUNICATION

Quantitative measurement of exchange dynamics in proteins via ^{13}C relaxation dispersion of $^{13}CHD_2$-labeled samples

Enrico Rennella[1] · Anne K. Schuetz[1] · Lewis E. Kay[1,2]

Received: 21 March 2016 / Accepted: 19 May 2016 / Published online: 1 June 2016

Abstract Methyl groups have emerged as powerful probes of protein dynamics with timescales from picoseconds to seconds. Typically, studies involving high molecular weight complexes exploit $^{13}CH_3$- or $^{13}CHD_2$-labeling in otherwise highly deuterated proteins. The $^{13}CHD_2$ label offers the unique advantage of providing ^{13}C, ^{1}H and ^{2}H spin probes, however a disadvantage has been the lack of an experiment to record ^{13}C Carr–Purcell–Meiboom–Gill relaxation dispersion that monitors millisecond time-scale dynamics, implicated in a wide range of biological processes. Herein we develop an experiment that eliminates artifacts that would normally result from the scalar coupling between ^{13}C and ^{2}H spins that has limited applications in the past. The utility of the approach is established with a number of applications, including measurement of ms dynamics of a disease mutant of a 320 kDa p97 complex.

Keywords CPMG · Conformational dynamics · Proteins · Methyl labeling · Relaxation dispersion · $^{13}CHD_2$

Electronic supplementary material The online version of this article (doi:10.1007/s10858-016-0038-9) contains supplementary material, which is available to authorized users.

✉ Lewis E. Kay
kay@pound.med.utoronto.ca

[1] Departments of Molecular Genetics, Biochemistry and Chemistry, University of Toronto, Toronto, ON M5S 1A8, Canada

[2] Program in Molecular Structure and Function, Hospital for Sick Children, 555 University Avenue, Toronto, ON M5G 1X8, Canada

Introduction

NMR spectroscopy has emerged as a very powerful technique for the study of protein dynamics over timescales that span many orders of magnitude (Mittermaier and Kay 2006). The development of optimal labeling schemes and the design of the appropriate experiments that exploit them have proven critical in extending applications to increasingly larger proteins and protein complexes (Pervushin et al. 1998; Tugarinov et al. 2003). One popular approach for studies of sidechain dynamics makes use of proteins that are highly deuterated, with methyl group probes labeled as either $^{13}CH_3$ or $^{13}CHD_2$ (Tugarinov and Kay 2005). Each different methyl labeling approach has unique and often complementary strengths. For example, the $^{13}CH_3$ label provides the greatest sensitivity for studies of high molecular weight protein systems in general, by exploiting a methyl-TROSY effect (Tugarinov et al. 2003), and also enables studies of both fast time scale dynamics (ps–ns) (Tugarinov et al. 2007) and ms motional processes (Korzhnev et al. 2004) using approaches that exploit the cross-correlated relaxation networks that manifest in this spin system (Werbelow and Grant 1977). The $^{13}CHD_2$ label presents ^{13}C, ^{1}H and ^{2}H spins for measurement of motion in the ps–ns regime (Ishima et al. 2001) and ^{13}C and ^{1}H spins for quantifying dynamics that are in the μs–ms range via a number of different $R_{1\rho}$-, CPMG- and CEST-types of experiments (Baldwin et al. 2010; Brath et al. 2006; Otten et al. 2010; Rennella et al. 2015).

A particularly important goal in protein dynamics studies by NMR is to characterize sparsely populated and transiently formed states that are generated via excursions from the populated, ground conformer, often the only state that is amenable to characterization using more 'routine' non-NMR biophysical measurements (Sekhar and Kay 2013).

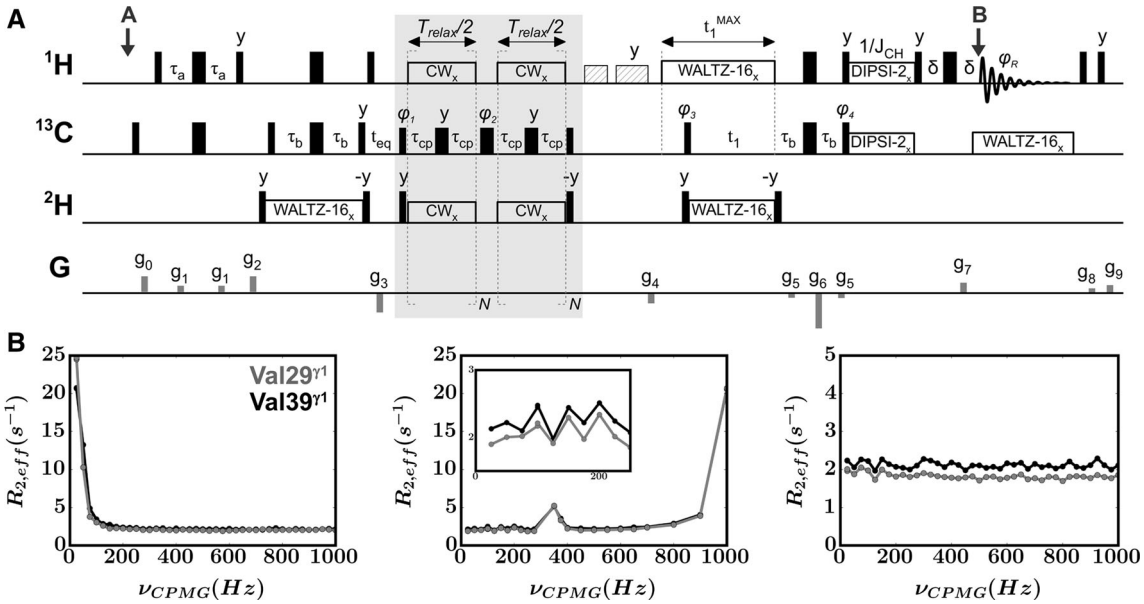

Fig. 1 **a** Pulse sequence for measurement of ^{13}C SQ CPMG relaxation dispersion profiles using $^{13}CHD_2$ spin systems. 90° (180°) pulses applied at maximum power are denoted by narrow (wide) *black bars* (with the exception of ^{13}C pulses in the shaded element where a 17 kHz field is used), with pulse phases assumed to be x unless otherwise indicated. Between points *A* and *B* the ^{1}H carrier is placed in the center of the methyl region (1 ppm), while at point *B* the carrier is jumped to the water line (4.7 ppm); ^{13}C and ^{2}H carriers are positioned at 20 ppm and 1 ppm, respectively. ^{1}H, ^{13}C and ^{2}H WALTZ-16 decoupling elements (Shaka et al. 1983) are applied with fields of 6.2, 2 kHz and 710 Hz, respectively. Continuous wave (CW) elements are applied during the constant-time CPMG element (Mulder et al. 2001) of duration T_{relax} for $N \neq 0$. A ^{1}H field of approximately 17 kHz is employed (Jiang et al. 2015), while for ^{2}H a field of approximately 1 kHz is used for $\nu_{CPMG} \leq 250$ Hz. The exact strength of the ^{2}H CW element, ν_{CW} (Hz), is adjusted to match the condition $\nu_{CW} = 2k \cdot \nu_{CPMG}$ (Vallurupalli et al. 2007) where k is a natural number. On our system heating is not observed with ^{2}H decoupling and thus no compensation is used for $\nu_{CPMG} > 250$ Hz. In contrast to ^{2}H, no adjustment is required for the ^{1}H CW field because a strong field is applied and the matching condition can be neglected (Jiang et al. 2015). For the case where $N = 0$ (reference plane) the ^{1}H CW element is applied immediately following data acquisition to ensure uniform heating, independent of the value of N. The two synchronous DIPSI-2 (Shaka et al. 1988) elements are employed for heteronuclear cross-polarization (8 ms) using a field of 8 kHz. Striped boxes indicate purge elements (3.6 kHz) of durations 2 (*x-axis*) and 3.4 ms (*y-axis*) for water suppression (Messerlie et al. 1989). The delays used are: $\tau_a = 1.8$ ms, $\tau_b = 2$ ms, $\tau_{cp} = T_{relax}/(4 \cdot N)$, t_1^{MAX} = maximum t_1 duration, $\delta = 460$ µs. The delay t_{eq} before the CPMG element (partially) restores equilibrium magnetization values, depending on the value of k_{ex}. The phase cycle is as follows: $\varphi_1 = x, -x$; $\varphi_2 = 4\{x\}, 4\{-x\}$; $\varphi_3 = 2\{y\}, 2\{-y\}$; $\varphi_4 = y$; $\varphi_R = x, -x, -x, x$. Quadrature detection in the indirect dimension is obtained using the gradient enhanced sensitivity approach (Kay et al. 1992; Schleucher et al. 1993) whereby separate data sets are recorded for each t_1 point with (φ_4, g6) and ($-\varphi_4$, −g6). Gradients are applied with the following durations (ms) and strengths (G/cm): g_0: (1, 21.4), g_1:(0.5, 16), g_2: (0.8, 26.8), g_3: (1, −26.8), g_4: (0.9, −16), g_5: (0.3, −21.4), g_6: (1.02, −48.2), g_7: (0.26, 48.2), g_8: (0.22, −16), g_9: (0.45, −16). The g_5 gradient pair is inverted with g_6. **b** Experimental CPMG profiles measured on GB1. (*left*) ^{2}H CW decoupling is not employed, (*center*) a constant 1 kHz ^{2}H CW field is used, (*right*) using a ^{2}H CW field with $\nu_{CW} = 2k \cdot \nu_{CPMG}$ (Vallurupalli et al. 2007) for $\nu_{CPMG} \leq 250$ Hz, $\nu_{CW} = 0$ for $\nu_{CPMG} > 250$ Hz, as in Fig. 2. A 16.7 kHz ^{1}H CW decoupling field is applied in all cases (Jiang et al. 2015)

A number of NMR experiments have been developed with this goal in mind, including those exploiting $^{13}CH_3$ and $^{13}CHD_2$ methyl probes. Notably, ^{13}C CEST-based experiments have been shown to be fivefold to sixfold more sensitive for $^{13}CHD_2$ methyl groups than for their $^{13}CH_3$ counterparts in an application involving the half proteasome that has a molecular mass of 360 kDa (Rennella et al. 2015). In addition, a ^{1}H-CPMG experiment has been developed for the measurement of ms time-scale dynamics in $^{13}CHD_2$-labeled proteins and applied to studies of proteasome gating (Baldwin et al. 2010). In contrast, corresponding single-quantum (SQ) based ^{1}H-CPMG experiments using fully protonated methyls are not possible unless magnetization from only $\frac{1}{2}$ manifolds is selected (Tugarinov and Kay 2007), since imperfections in CPMG refocusing pulses lead to artifacts that interfere with the quantification of relaxation dispersion profiles (Korzhnev et al. 2005). Despite these advantages, a significant drawback with using the $^{13}CHD_2$ label for studies of slow dynamics relates to the fact that it has not been possible to record ^{13}C-CPMG dispersion profiles over the complete range of ^{13}C pulsing frequencies that are often necessary to fully characterize such exchanging systems (Ishima et al. 1999). This is especially problematic for systems where the exchange rate is relatively slow (on the order of several hundreds/s). At the heart of the problem lies an interference effect resulting from the 'combined action' of the one-bond ^{13}C–^{2}H scalar couplings and the rapid ^{2}H spin–lattice

relaxation in such systems that can severely distort dispersion profiles (see below). Herein we present a ^{13}C-SQ CPMG pulse scheme for studies of chemical exchange using $^{13}CHD_2$ methyls that eliminates this problem. The robustness of the experiment is established and its utility demonstrated with an application to the measurement of exchange dynamics in a 320 kDa construct of p97, a protein that plays a major role in cellular homeostasis (Braun and Zischka 2008).

Figure 1 shows the pulse sequence that has been developed for measurement of ^{13}C SQ CPMG relaxation dispersion profiles using $^{13}CHD_2$ spin systems, where T_{relax} is the CPMG interval for recording effective ^{13}C transverse relaxation rates, $R_{2,eff}$, as a function of the frequency of application of ^{13}C chemical shift refocusing pulses, ν_{CPMG}. During this period a ^{1}H continuous wave (CW) decoupling field is applied at high strength ($\geq$15 kHz) (Jiang et al. 2015), ensuring that ^{13}C magnetization remains in-phase with respect to the coupled ^{1}H spin in the $^{13}CHD_2$ methyl. This eliminates the effects of imbalance in relaxation rates of in-phase and anti-phase ^{13}C magnetization (with respect to ^{1}H) that can give rise to spurious dispersion profiles. The ^{13}C–^{2}H scalar coupled evolution of ^{13}C magnetization during the CPMG interval can also lead to a ν_{CPMG} dependent contribution to the dispersion profile that is independent of chemical exchange, complicating extraction of robust exchange parameters. This is illustrated by an application to a sample of the B1 domain from immunoglobulin binding protein G (GB1). GB1 does not show ms time-scale dynamics in other experiments (Korzhnev et al. 2005), yet pathologic dispersion profiles are observed for all residues using the scheme of Fig. 1 when ^{2}H decoupling is not applied during the CPMG interval, Fig. 1b (left). These 'erroneous' profiles, showing large $R_{2,eff}$ rates at low CPMG pulsing frequencies, result from ^{13}C–^{2}H scalar coupled evolution of ^{13}C magnetization in concert with ^{2}H longitudinal relaxation that effectively interconverts the ^{13}C multiplet components as they evolve (Abragam 1961; Grzesiek et al. 1993). For $\nu_{CPMG} \geq 250$ Hz the attached deuterons are effectively decoupled and this region of the resulting dispersion profile is thus flat in the absence of exchange. Application of a uniform 1 kHz CW ^{2}H decoupling field improves performance at the low CPMG frequency end but artifacts are predicted when $\nu_{CW} = (2k - 1)\cdot\nu_{CPMG}$, where ν_{CW} is the strength of the ^{2}H CW field in Hz and k is a natural number. As can be seen in Fig. 1b (middle) large spikes in $R_{2,eff}$ values are observed at 350 Hz ($k = 2$) and 1 kHz ($k = 1$), as predicted, as well as smaller spikes for $k > 2$ (inset). These arise when the centers of the ^{13}C and ^{2}H pulses coincide, leading to evolution of ^{13}C-^{2}H scalar coupling during T_{relax}. In contrast, when a ^{2}H decoupling scheme is used such that $\nu_{CW} = 2k\cdot\nu_{CPMG}$ for $\nu_{CPMG} \leq 250$ Hz (Vallurupalli et al. 2007) and 'no field' for $\nu_{CPMG} > 250$ Hz, flat dispersion profiles are obtained over the complete ν_{CPMG} range, Fig. 1b (right). Here we have kept the ^{2}H CW field close to 1 kHz, with changes $\sim\pm$ 10 % for different ν_{CPMG} rates to ensure that $\nu_{CW} = 2k\cdot\nu_{CPMG}$, Fig. 2. The required power levels for the ^{2}H CW decoupling field as a function of ν_{CPMG} can be calculated using a C-based program that is provided in Supporting Information and by the authors upon request.

Having established a robust experimental scheme for recording ^{13}C dispersion profiles in $^{13}CHD_2$ labeled proteins we next recorded experiments on a sample of an Ile, Leu, Val $^{13}CHD_2$-labeled G48A Fyn SH3 domain that interconverts between a highly populated native, folded conformation and a sparsely populated ensemble that corresponds to the unfolded state. The insets in Fig. 3 show ^{13}C dispersion profiles for Leu $29^{\delta 2}$ and Val $55^{\gamma 2}$ recorded with the pulse scheme of Fig. 1. Profiles from all residues have been fit simultaneously to a two state model of chemical exchange, $G \underset{k_{EG}}{\overset{k_{GE}}{\rightleftarrows}} E$, where G and E denote ground and excited states, respectively. Extracted exchange parameters, $k_{ex} = 104 \pm 2$ s^{-1}, $p_E = 10.0 \pm 0.2$ % (25 °C), where p_E is the fractional population of the rare state, are in excellent agreement with those obtained previously from ^{13}C CEST, $k_{ex} = 105 \pm 2$ s^{-1}, $p_E = 9.5 \pm 0.1$ %. Further verification of the methodology can be obtained by comparing the extracted chemical shifts, $|\Delta\varpi|$ (ppm), between the exchanging states obtained from the present study with those from ^{13}C-CEST, Fig. 3, and the agreement is excellent.

We were interested in comparing the sensitivity of the present scheme with previously published methods for

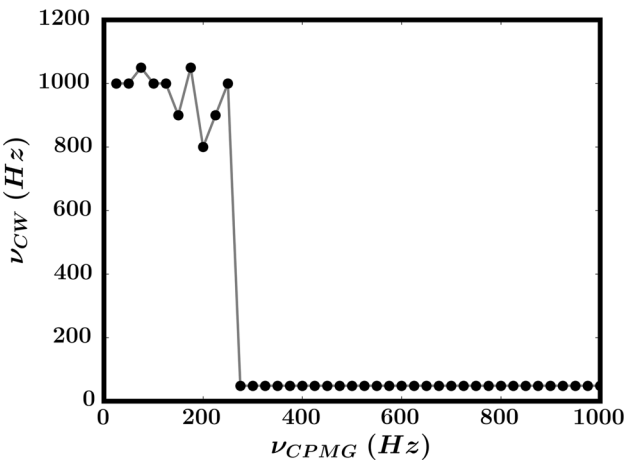

Fig. 2 Modulation of the ^{2}H CW decoupling field (ν_{CW}) as a function of ν_{CPMG} to ensure that the condition $\nu_{CW} = 2k\cdot\nu_{CPMG}$ is satisfied for $\nu_{CPMG} \leq 250$ Hz (see Fig. 1b, right). An approximate 1 kHz ^{2}H decoupling field is chosen. See Supporting Information for C-code used to generate power levels for ^{2}H CW decoupling

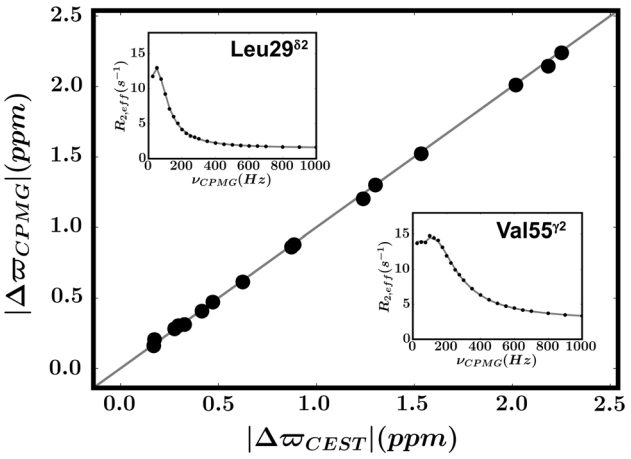

Fig. 3 Linear correlation plot of extracted chemical shifts, $|\Delta\varpi|$ (ppm), obtained from analysis of ^{13}C SQ dispersion profiles recorded on a $^{13}CHD_2$-sample of the G48A Fyn SH3 domain, 25 °C (*y-axis*) with those from analysis of a ^{13}C-CEST dataset obtained under identical conditions (Rennella et al. 2015). *Insets* show a pair of methyl dispersion profiles, 600 MHz, recorded with the scheme of Fig. 1

recording ^{13}C CPMG profiles of $^{13}CH_3$-labeled proteins, focusing in particular on high molecular weight complexes. To this end we have compared spectra recorded on the half proteasome, $\alpha_7\alpha_7$, from *T. Acidophilum* (Sprangers and Kay 2007), labeled as [U-^{2}H; Ileδ1-$^{13}CH_3$; Leu, Val-$^{13}CH_3$/$^{12}CD_3$; Met-$^{13}CH_3$] or [U-^{2}H; Ileδ1-$^{13}CHD_2$; Leu,Val-$^{13}CHD_2$/$^{13}CHD_2$; Met-$^{13}CH_3$]. The $\alpha_7\alpha_7$ complex has an aggregate molecular mass of 360 kDa and an estimated overall tumbling time of 125 ns at 50 °C (Sprangers and Kay 2007). Figure 4 plots signal-to-noise (S/N) values as a function of methyl group for CPMG spectra recorded with $T_{relax} = 25$ ms, 50 °C, using a methyl-TROSY scheme (Korzhnev et al. 2004) (black squares, $^{13}CH_3$-labeled protein), the present pulse sequence (dark grey circles, $^{13}CHD_2$-labeling) and a previously published ^{13}C SQ-based experiment that was intended for studies of small to medium sized proteins (Lundstrom et al. 2007) (light grey diamonds, $^{13}CH_3$). As expected the methyl-TROSY scheme provides the best sensitivity (by roughly a factor of 2-3, on average, over the SQ $^{13}CHD_2$ experiment), with the SQ $^{13}CHD_2$ version significantly better than its SQ $^{13}CH_3$ counterpart. It is clear that from the point of view of sensitivity, often limiting in applications involving high molecular weight proteins, that the methyl-TROSY scheme is advantageous.

Despite the sensitivity loss in comparison to the methyl-TROSY experiment there is an advantage with the $^{13}CHD_2$-scheme. As discussed previously, methyl-TROSY CPMG profiles are sensitive to both ^{13}C and ^{1}H chemical shift differences between spins in the exchanging states (Korzhnev et al. 2004). This offers the appealing possibility of obtaining *both* ^{13}C and ^{1}H methyl chemical shifts of the rare conformer from a single experiment. However, in practice it can be difficult to simultaneously obtain accurate $\Delta\varpi$ values for both ^{13}C and ^{1}H, unless S/N is high, and experiments that probe one $\Delta\varpi$ value at a time, as is possible for $^{13}CHD_2$- but not for $^{13}CH_3$-labeled samples using the methyl-TROSY approach (Korzhnev et al. 2005), can thus be desirable. By means of illustration, we have carried out simulations showing that while similar errors in ^{13}C $\Delta\varpi$ values are obtained from fits of SQ and methyl-TROSY data when ^{1}H $\Delta\varpi = 0$, fitted shift parameters from methyl-TROSY dispersions can become less accurate as ^{1}H shift differences increase because dispersion size correlates inversely with the magnitude of ^{1}H $\Delta\varpi$ (Fig. S1). For example, ^{13}C SQ CPMG dispersion profiles that are on the order of 5–10 s^{-1} for $^{13}CH_3$-labeled G48A Fyn SH3 decrease significantly (to $\sim$2–3 s^{-1}) in methyl-TROSY CPMG data sets, making it challenging to extract accurate ^{13}C $\Delta\varpi$ values from fits. This emphasizes the tradeoff between high sensitivity (methyl-TROSY) and robustness of data fitting that is higher in the SQ experiment where dispersion profiles are insensitive to ^{1}H $\Delta\varpi$.

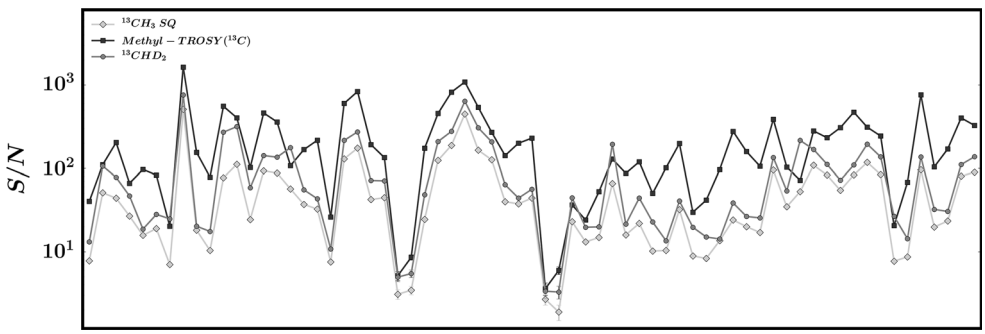

Fig. 4 S/N as a function of methyl group for CPMG spectra recorded on $^{13}CHD_2$- and $^{13}CH_3$-labeled $\alpha_7\alpha_7$ samples, with $T_{relax} = 25$ ms, 50 °C. S/N ratios obtained using a methyl-TROSY scheme (Korzhnev et al. 2004) (*black squares* $^{13}CH_3$-labeled protein), the present pulse sequence (*dark grey circles* $^{13}CHD_2$-labeling) and a previously published ^{13}C SQ-based experiment (Lundstrom et al. 2007) (*light grey diamonds* $^{13}CH_3$) are plotted

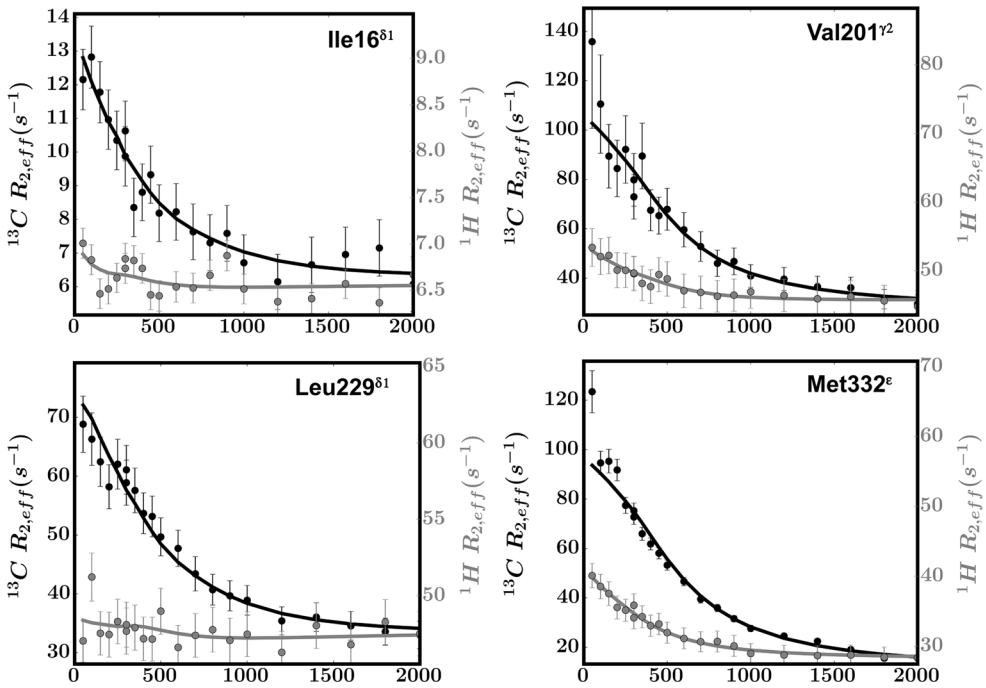

Fig. 5 Experimental ^{13}C (*black*) and ^{1}H (*grey*) CPMG profiles (*circles*) measured on a 0.6 mM sample of $^{13}CHD_2$-methyl labeled R95G p97, 50 °C, 800 MHz, together with fits of dispersion profiles to a two-site exchange model using the Bloch–McConnell equations (McConnell 1958) (*solid lines*). Details are provided in Supporting Information

Figure 5 shows selected ^{13}C and ^{1}H SQ dispersion profiles recorded on a [U-^{2}H; Ileδ1-$^{13}CHD_2$; Leu, Val-$^{13}CHD_2$/$^{13}CHD_2$; Met-$^{13}CHD_2$]-labeled sample of an R95G mutant of p97. Notably, both ^{13}C and ^{1}H profiles can be recorded on a single sample. The p97 protein is a ubiquitous ATPase, comprising ~1 % of the total protein in the cell (Song et al. 2003), with the R95G mutation responsible for a neurodegenerative disease that leads to dementia (Kimonis et al. 2008). To address the role of dynamics in p97 function/misfunction we have recorded ^{13}C/^{1}H CPMG dispersion profiles of this protein. An extensive conformational exchange process has been discovered involving residues at domain interfaces that can be fit globally to a two-site exchange model with $k_{ex} = 2300 \pm 400\ s^{-1}$.

In summary, we have presented an experiment for recording ^{13}C SQ CPMG dispersion profiles of $^{13}CHD_2$-labeled proteins. Artifacts that normally result from the presence of coupled deuterons are eliminated using a ^{2}H decoupling field that varies as a function of ν_{CPMG}. The utility of the approach has been established through tests on small proteins, showing the expected flat dispersion profiles where there is no exchange, while correct exchange parameters are fit for systems that interconvert. Although the $^{13}CHD_2$-based experiment is significantly less sensitive than the methyl-TROSY CPMG scheme, it can offer advantages with regards to robustness of extracted chemical shift parameters, and the $^{13}CHD_2$-labeling does offer the possibility of performing a wide range of different (^{1}H, ^{13}C, ^{2}H) relaxation measurements. Notably, high quality data can be obtained on a 320 kDa fragment of p97. The $^{13}CHD_2$-CPMG experiment, in concert with a previously published ^{1}H-CPMG scheme for $^{13}CHD_2$-labeled proteins (Baldwin et al. 2010), enables accurate measurement of both ^{1}H and ^{13}C chemical shifts of rare protein conformers that will provide an important starting point for characterizing how these states are involved in biological function.

Acknowledgments A.K.S is the recipient of an EMBO Long Term Fellowship and an Early Postdoc Mobility Fellowship from the Swiss National Science Foundation. This work was funded through a Canadian Institute of Health Research grant to L.E.K. L.E.K. holds a Canada Research Chair in Biochemistry.

References

Abragam A (1961) Principles of nuclear magnetism. Clarendon Press, Oxford

Baldwin AJ, Religa TL, Hansen DF, Bouvignies G, Kay LE (2010) $^{13}CHD_2$ methyl group probes of millisecond time scale exchange in proteins by ^{1}H relaxation dispersion: an application to proteasome gating residue dynamics. J Am Chem Soc 132: 10992–10995. doi:10.1021/ja104578n

Brath U, Akke M, Yang D, Kay LE, Mulder FA (2006) Functional dynamics of human FKBP12 revealed by methyl ^{13}C rotating frame relaxation dispersion NMR spectroscopy. J Am Chem Soc 128:5718–5727. doi:10.1021/ja0570279

Braun RJ, Zischka H (2008) Mechanisms of Cdc48/VCP-mediated cell death: from yeast apoptosis to human disease. Biochim Biophys Acta 1783:1418–1435. doi:10.1016/j.bbamcr.2008.01.015

Grzesiek S, Anglister J, Ren H, Bax A (1993) ^{13}C line narrowing by 2H decoupling in ^{2}H/^{13}C/^{15}N-enriched proteins. Applications to triple resonance 4D J-connectivity of sequential amides. J Am Chem Soc 115:4369–4370

Ishima R, Louis JM, Torchia DA (1999) Transverse ^{13}C relaxation of CHD_2 methyl isotopomers to detect slow conformational changes of protein side chains. J Am Chem Soc 121:11589–11590

Ishima R, Petkova AP, Louis JM, Torchia DA (2001) Comparison of methyl rotation axis order parameters derived from model-free analyses of ^{2}H and ^{13}C longitudinal and transverse relaxation rates measured in the same protein sample. J Am Chem Soc 123:6164–6171

Jiang B, Yu B, Zhang X, Liu M, Yang D (2015) A ^{15}N CPMG relaxation dispersion experiment more resistant to resonance offset and pulse imperfection. J Magn Reson 257:1–7. doi:10.1016/j.jmr.2015.05.003

Kay LE, Keifer P, Saarinen T (1992) Pure absorption gradient enhanced heteronuclear single quantum correlation spectroscopy with improved sensitivity. J Am Chem Soc 114:10663–10665

Kimonis VE, Fulchiero E, Vesa J, Watts G (2008) VCP disease associated with myopathy, Paget disease of bone and frontotemporal dementia: review of a unique disorder. Biochim Biophys Acta 1782:744–748. doi:10.1016/j.bbadis.2008.09.003

Korzhnev DM, Kloiber K, Kanelis V, Tugarinov V, Kay LE (2004) Probing slow dynamics in high molecular weight proteins by methyl-TROSY NMR spectroscopy: application to a 723-residue enzyme. J Am Chem Soc 126:3964–3973

Korzhnev DM, Mittermaier AK, Kay LE (2005) Cross-correlated spin relaxation effects in methyl ^{1}H CPMG-based relaxation dispersion experiments: complications and a simple solution. J Biomol NMR 31:337–342. doi:10.1007/s10858-005-2468-7

Lundstrom P, Vallurupalli P, Religa TL, Dahlquist FW, Kay LE (2007) A single-quantum methyl ^{13}C-relaxation dispersion experiment with improved sensitivity. J Biomol NMR 38:79–88

McConnell HM (1958) Reaction rates by nuclear magnetic resonance. J Chem Phys 28:430–431

Messerlie BA, Wider W, Otting G, Weber C, Wuthrich K (1989) Solvent suppression using a spin lock in 2D and 3D NMR spectroscopy with H_2O solutions. J Magn Reson 85:608–612

Mittermaier A, Kay LE (2006) New tools provide new insights in NMR studies of protein dynamics. Science 312:224–228

Mulder FAA, Skrynnikov NR, Hon B, Dahlquist FW, Kay LE (2001) Measurement of slow timescale dynamics in protein sidechains by ^{15}N relaxation dispersion NMR spectroscopy: application to Asn and Gln Residues in a Cavity Mutant of T4 lysozyme. J Am Chem Soc 123:967–975

Otten R, Villali J, Kern D, Mulder FA (2010) Probing microsecond time scale dynamics in proteins by methyl ^{1}H Carr–Purcell–Meiboom–Gill relaxation dispersion NMR measurements. Application to activation of the signaling protein NtrC(r). J Am Chem Soc 132:17004–17014. doi:10.1021/ja107410x

Pervushin K, Riek R, Wider G, Wüthrich K (1998) Transverse relaxation-optimized spectroscopy (TROSY) for NMR studies of aromatic spin systems in ^{13}C-labeled proteins. J Am Chem Soc 120:6394–6400

Rennella E, Huang R, Velyvis A, Kay LE (2015) $^{13}CHD_2$-CEST NMR spectroscopy provides an avenue for studies of conformational exchange in high molecular weight proteins. J Biomol NMR 63:187–199. doi:10.1007/s10858-015-9974-z

Schleucher J, Sattler M, Griesinger C (1993) Coherence selection by gradients without signal attenuation: application to the three-dimensional HNCO experiment. Angew Chem Int Ed Engl 32:1489–1491

Sekhar A, Kay LE (2013) NMR paves the way for atomic level descriptions of sparsely populated, transiently formed biomolecular conformers. Proc Natl Acad Sci USA 110:12867–12874. doi:10.1073/pnas.1305688110

Shaka AJ, Keeler J, Frenkiel T, Freeman R (1983) An improved sequence for broadband decoupling: WALTZ-16. J Magn Reson 52:335–338

Shaka AJ, Lee CJ, Pines A (1988) Iterative schemes for bilinear operators—application to spin decoupling. J Magn Reson 77:274–293

Song C, Wang Q, Li CC (2003) ATPase activity of p97-valosin-containing protein (VCP). D2 mediates the major enzyme activity, and D1 contributes to the heat-induced activity. J Biol Chem 278:3648–3655. doi:10.1074/jbc.M208422200

Sprangers R, Kay LE (2007) Quantitative dynamics and binding studies of the ^{20}S proteasome by NMR. Nature 445:618–622

Tugarinov V, Kay LE (2005) Methyl groups as probes of structure and dynamics in NMR studies of high-molecular-weight proteins. ChemBioChem 6:1567–1577

Tugarinov V, Kay LE (2007) Separating degenerate 1(H) transitions in methyl group probes for single-quantum (1)H-CPMG relaxation dispersion NMR spectroscopy. J Am Chem Soc 129:9514–9521

Tugarinov V, Hwang P, Ollerenshaw J, Kay LE (2003) Cross-correlated relaxation enhanced ^{1}H–^{13}C NMR spectroscopy of methyl groups in very high molecular weight proteins and protein complexes. J Am Chem Soc 125:10420–10428

Tugarinov V, Sprangers R, Kay LE (2007) Probing side-chain dynamics in the proteasome by relaxation violated coherence transfer NMR spectroscopy. J Am Chem Soc 129:1743–1750

Vallurupalli P, Scott L, Williamson JR, Kay LE (2007) Strong coupling effects during X-pulse CPMG experiments recorded on heteronuclear ABX spin systems: artifacts and a simple solution. J Biomol NMR 38:41–46

Werbelow LG, Grant DM (1977) Intramolecular dipolar relaxation in multispin systems. Adv Magn Reson 9:189–299